STEM CELLS TRANSLATIONAL MEDICINE®

TISSUE ENGINEERING AND REGENERATIVE MEDICINE

The Lymph Node as a New Site for Kidney Organogenesis

MARIA GIOVANNA FRANCIPANE,[a,b] ERIC LAGASSE[a]

Key Words. Kidney • Organogenesis • Lymph node • Bioreactor • Stem cells

[a]Department of Pathology, McGowan Institute for Regenerative Medicine, University of Pittsburgh School of Medicine, Pittsburgh, Pennsylvania, USA; [b]Ri.MED Foundation, Palermo, Italy

Correspondence: Eric Lagasse, Pharm.D., Ph.D., 450 Technology Drive, Suite 300, Pittsburgh, Pennsylvania 15219, USA. Telephone: 412-624-5285; E-Mail: Lagasse@pitt.edu

Received September 18, 2014; accepted for publication December 23, 2014; first published online in SCTM *EXPRESS* February 2, 2015.

1066-5099/2015/$20.00/0

http://dx.doi.org/10.5966/sctm.2014-0208

ABSTRACT

The shortage of organs for kidney transplantation has created the need to develop new strategies to restore renal structure and function. Given our recent finding that the lymph node (LN) can serve as an in vivo factory to generate or sustain complex structures like liver, pancreas, and thymus, we investigated whether it could also support kidney organogenesis from mouse renal embryonic tissue (metanephroi). Here we provide the first evidence that metanephroi acquired a mature phenotype upon injection into LN, and host cells likely contributed to this process. Urine-like fluid-containing cysts were observed in several grafts 12 weeks post-transplantation, indicating metanephroi transplants' ability to excrete products filtered from the blood. Importantly, the kidney graft adapted to a loss of host renal mass, speeding its development. Thus, the LN might provide a unique tool for studying the mechanisms of renal maturation, cell proliferation, and fluid secretion during cyst development. Moreover, we provide evidence that inside the LN, short-term cultured embryonic kidney cells stimulated with the Wnt agonist R-Spondin 2 gave rise to a monomorphic neuron-like cell population expressing the neuronal 200-kDa neurofilament heavy marker. This finding indicates that the LN might be used to validate the differentiation potential of candidate stem cells in regenerative nephrology. STEM CELLS TRANSLATIONAL MEDICINE *2015;4:295–307*

INTRODUCTION

There are nearly 400,000 end-stage renal disease (ESRD) patients in the U.S. and approximately 2,000,000 worldwide, increasing 4%–5% annually [1]. All ESRD patients need dialysis or transplantation to stay alive, and a severe organ shortage is driving research for alternative therapies.

Although stem cell-based therapies have been proposed as a solution to restore structural and functional integrity of injured tissues, these approaches may not be possible when the native environment is diseased or not readily accessible. Ectopic organogenesis can be an alternative approach to provide compensatory function for the damaged organ [2, 3]. Unfortunately, although several extravascular and a few immunoprivileged sites have been considered as potential ectopic transplantation sites for organs like pancreas [4] and liver [5], ectopic sites for kidney reconstruction have not yet been fully examined.

Renal capsule grafting is a well-established method of growing rudimentary organs in vivo for extended periods [6]. It was speculated that developing nephrons implanted beneath the renal capsule might become incorporated into the collecting system of the host and thereby increase host renal function [6]. However, such incorporation and consequent enhancement of renal function have never been demonstrated for isotranplants, allotransplants, or xenotransplants [6]. In addition, space limitation beneath the renal capsule has proven to be an impediment to the growth of transplants [6]. More importantly, even assuming that metanephroi transplantation beneath the renal capsule could effectively enhance renal function in the animal, it could not be considered clinically realistic, because the human kidney capsule and parenchyma cannot be easily separated like in rodents to permit cell transplantation [7]. The omentum also provides a favorable environment for organogenesis [8]. Hammerman's group first suggested that whole rat metanephroi implanted into the omentum might enlarge, become vascularized, and form mature tubules and glomeruli [9]. However, other studies showed that transplanted metanephroi can grow and develop for only a short time in the host omentum [10], unless an end-to-end anastomosis to the host ureters is performed [11]. Only a few reports have shown that it is technically feasible to microsurgically connect donor and host ureters. In these studies, ureteroureterostomy slowed the progression of kidney failure in nephrectomized animals [12], prolonged short-term survival of anephric rats [11], or caused a rise in blood pressure in acutely hypotensive rats [13]. Although promising, these results point to several limitations in the clinic that also include postoperative adhesions and intestinal obstruction following omental manipulation [14, 15]. The anterior chamber of live rodent eyes has also been used

as a site to transplant differently staged whole embryonic kidneys [16, 17] or cultured fetal kidney cells [18]. However, these studies failed to demonstrate long-term graft acceptance. Although glomerular and tubular differentiation could occur in implants of whole kidneys, signs of graft rejection were observed in most samples by 16 days after in oculo implantation [16]. A more recent study, however, showed that acapsular glomeruli transplanted into the anterior chamber of the mouse eye preserve their structure and function for at least 6 months after transplantation [19]. Nevertheless, morphological analysis of these glomeruli was hampered by the low efficiency of transplantation. Indeed, only a fraction of transplanted glomeruli engrafted (1–3 per eye), and only 10% of them completely reperfused. Therefore, the eye chamber does not fully meet all criteria to be considered an effective transplantation site, and it is clinically impractical for potential kidney reconstruction. Conversely, our previous findings indicate that the lymph node (LN) might be a clinically relevant site for transplantation [20–22]. First, there are over 500 LNs in the human body, many of which are relatively easily accessible. Second, although a single LN structurally limits the number of donor cells that can be transplanted, it is technically feasible to transplant more than one LN to gain sufficient organ or tissue function from the transplanted cells. Third, LNs have ready access to the bloodstream, which nurtures cells with nutrients, as well as hormones and signaling agents needed for growth. Importantly, new angiogenesis occurs fast enough in this site to sustain cell survival and engraftment. All these characteristics allowed us to generate functional liver, thymus, and pancreatic islets within the mouse LN [20, 21].

As an extension of our previous findings, we attempted to grow a kidney within the LN. Here, we show that the LN allowed mouse metanephroi to engraft and mature as well as recruited host bone marrow-derived cells to the transplant. Healthy nephrons could be found until the 12th week post-transplantation. Production of fluid waste over time seemed to result in graft degeneration. Importantly, kidney ectopic grafts adapted to a loss of host renal mass with accelerated development. Finally, we suggest that LNs might be used to study regulation of lineage decisions and functional specialization from cells with stem/progenitor features.

Materials and Methods

Animals

All mice were purchased from the Jackson Laboratory (Bar Harbor, ME, http://www.jax.org), bred, and housed in the Division of Laboratory Animal Resources facility at the University of Pittsburgh. Experimental protocols followed U.S. NIH guidelines for animal care and were approved by the University of Pittsburgh Institutional Animal Care and Use Committee.

Tissue Collection, Cell Culture, and Transplantation

Embryonic day (E) 14–15.5 kidneys were retrieved from timed pregnant green fluorescent protein $(GFP)^+$ or wild-type (wt) C57BL/6 mice under a dissecting microscope (embryos were considered 0.5 days old when a vaginal plug was detected in the morning). For renal fragment transplantation, kidneys were minced in PBS and kept on ice until injection ($n = 43$, kidneys from one embryo per recipient mouse). For transplantation of freshly isolated cell suspensions, kidneys were rapidly dissociated with 0.25% trypsin-EDTA, filtered through a 40-μm mesh, and injected as a cell/Matrigel suspension ($n = 11$, 10^6 cells per recipient mouse). Alternatively, kidney cells were plated onto a confluent layer of lethally irradiated LA7 feeder cells in Dulbecco's modified Eagle's medium/F-12 containing 1% insulin-transferrin-selenium, 0.5% fetal bovine serum, and 25 mg/ml gentamicin. Cells were treated for 7 days with or without 100 ng/ml R-Spondin 2 (RSPO2; catalog no. 3266-RS; R&D Systems Inc., Minneapolis, MN, http://www.rndsystems.com) or a combination of 3 μM CHIR99021 (catalog no. 4423; Tocris Bioscience, Bristol, U.K., http://www.tocris.com) and 1 μM TTNPB ((E)-4-[2-(5,6,7,8-tetrahydro-5,5,8,8-tetramethyl-2-naphthylenyl)-1-propenyl] benzoic acid; catalog no. 0761; Tocris Bioscience). Cells were then detached, counted, and injected in recipient mice as a cell/Matrigel suspension ($n = 2$/group, 2×10^5 cells per recipient mouse).

For LN transplantation, 6-week-old wt C57BL/6 mice ($n = 68$) were anesthetized with 1%–3% isoflurane. A small incision was made in the abdomen to expose jejunal LNs. Kidney fragments were slowly injected with a 1,000-μl threaded plunger syringe (catalog no. 81341; Hamilton Co., Reno, NV, http://www.hamiltoncompany.com) and a 20-gauge removable needle. Single cells were injected using a 25-μl gas-tight syringe (catalog no. 7656-01; Hamilton) and a 27-gauge removable needle (catalog no. 7803-01; Hamilton). Incisions were cauterized and sutured. Ketoprofen (2 mg/kg, i.m.) was then administered for 2 days to relieve postoperative pain. The mice were euthanized for analysis at predefined time points.

Histological Analyses and Immunostainings

Repopulated LNs and native kidneys were fixed in 4% paraformaldehyde and embedded in Tissue-Tek O.C.T. (Sakura Finetek, Tokyo, Japan, http://www.sakura-finetek.com) or paraffin for further analysis. Kidney cells were transferred onto microscopic slides, air-dried, and fixed in cold acetone, prior to immunocytochemistry.

Hematoxylin and eosin (H&E), periodic acid-Schiff (PAS), Masson's trichrome (TRI), and Picrosirius red (PSR) stains were performed on paraffin sections as described elsewhere. For bromodeoxyuridine (BrdU) staining, sections were incubated in 2 N HCl for 30 minutes to denature DNA, followed by 0.1 M borate buffer (pH 8.0) for 5 minutes for acid neutralization. All other stainings were performed according to standard procedures. Isotype-matched antibodies were used as negative controls. Supplemental online Table 1 indicates antibodies used.

Blood Urea Nitrogen Test

Blood urea nitrogen testing was performed on both mouse serum and LN fluid 16 weeks after kidney injection ($n = 5$ experimental mice, plus $n = 1$ control mouse). Serum samples were obtained by high-speed centrifugation of blood into serum-gel separator tubes (Terumo Medical Somerset, NJ, http://www.terumomedical.com). LN GFP^+ areas were identified and isolated under a fluorescent microscope, finely minced, and centrifuged at maximum speed for 10 minutes to collect the associated fluid. Blood urea nitrogen testing was performed using the QuantiChrom urea assay kit (catalog no. DIUR-500; Bioassay Systems, Hayward, CA, https://www.bioassaysys.com) according to the manufacturer's instructions.

Generation of Chimeric Mice

Bone marrow cells were harvested from the tibias and femurs of a GFP^+ C57BL/6 mouse, as described elsewhere. Subsequently,

6-week-old wt C57BL/6 mice ($n = 11$) were lethally irradiated and retro-orbitally infused immediately with 10^6 donor cells. Mice were treated with sulfamethoxazole in the drinking water.

Flow Cytometry

Mouse blood was collected from the submandibular facial vein. Flow cytometric analysis was performed using a MACSQuant (Miltenyi Biotec, Bergisch Gladbach, Germany, http://www.miltenyibiotec.com) and FlowJo software (Tree Star, Ashland, OR, http://www.treestar.com) according to standard procedures.

Left Nephrectomy and In Vivo Cell Proliferation Assay

To assess ectopic kidney development in response to growth stimuli, 12 days after kidney transplantation, mice underwent either a nephrectomy ($n = 5$) or sham operation ($n = 4$). Following a left-flank incision, the entire left kidney was exposed, and the infrarenal aorta and inferior vena cava were tied off with sutures. The kidney was excised immediately beyond the ligatures, and the incision was sutured. All mice were given drinking water containing 0.8 mg/ml BrdU immediately after surgery for 9 consecutive days. BrdU-containing water was freshly prepared daily. Regular water was reintroduced on day 10. All mice were euthanized for analysis after an additional 5 days. The number of $BrdU^+$-proliferating cells was assessed in native and ectopic kidneys.

Statistical Analysis

The data are presented as means $\pm$ SD. Statistical analysis was performed using Student's t test ($p < .05$ was considered significant).

RESULTS

The Lymph Node Is a Permissive Site for Kidney Organogenesis

We first investigated whether mid-embryonic mouse kidneys could integrate into a host mouse LN and undergo morphological maturation. Renal tissues were harvested from C57BL/6 GFP^+ embryos, isolated from ureteric buds, minced, and injected directly into jejunal LNs of adult wt C57BL/6 mice (Fig. 1A). After 3 weeks, recipient mice were sacrificed, and the LNs were collected and histologically examined. Morphogenesis of S-shaped bodies into more mature renal corpuscles was observed in these grafts (Fig. 1B). Developing renal corpuscles expressed type IV collagen in their glomerular basement membranes, as well as in mesangial areas (Fig. 1C). Three stages of glomerular maturation could be distinguished based on the literature (Fig. 1C) [23]. Importantly, fully mature glomeruli contained different cell types present in adult glomeruli, including $CD31^+$ endothelial cells, and $podoplanin^+$ podocytes (Fig. 1D). Developing kidneys also showed $claudin\text{-}2^+$ and $cytokeratin\text{-}8^+$ rudimentary tubules, as well as erythropoietin tubular expression, indicating hormonal competence (Fig. 1D; additional erythropoietin staining pictures are shown in supplemental online Fig. 1A). However, ectopic grafts continued to show a few S-shaped bodies, indicating incomplete maturation at the time of LN collection (Fig. 1C).

Kidney organogenesis within the LN was critically dependent on the renal development stage at the time of transplantation. Although 3-day-old mouse (P3) kidneys show glomerular maturity, they failed to efficiently engraft into the LN. At 3 weeks post-transplantation, E14–15.5 kidneys generated larger and thicker grafts compared with P3 kidneys (supplemental online Fig. 2). Moreover, although embryonic kidneys acquired more mature morphological characteristics within the LN, newborn kidneys failed to regenerate their native morphology, resulting in an imperfect glomerulogenesis (supplemental online Fig. 2). Prolonging the newborn kidney LN grafts for 12 weeks still did not result in better engraftment and maturation (data not shown), confirming the idea that embryonic kidneys harbor more regenerative potential than newborn kidneys.

Ectopic Grafts Show a Time-Dependent Functional Maturation

Three weeks after transplantation, it was not possible to confirm the presence of mature, functional nephrons. However, some mature nephrons were distinguishable in 6-week grafts (supplemental online Fig. 3A). Segments of renal tubule attached to developed renal corpuscles were observed. Furthermore, erythrocyte presence inside the capillary tuft of these elongated structures indicated probable blood filtration ability (supplemental online Fig. 3A). BrdU administered 24 hours prior to mouse sacrifice showed occasional proliferating cells within the ectopic glomeruli (supplemental online Fig. 3B). Reverse transcription (RT)-polymerase chain reaction (PCR) analysis for the presence of different urea transporter (UT-A1, UT-A2, UT-A3, and UT-B) mRNAs was performed in these grafts. UT-A transporters immunoreactivity appears first on E16. At this stage, however, UT-A levels are negligible and will strongly increase after birth [24]. Interestingly, we found all UT-A family members analyzed to be expressed at the mRNA level in 6-week grafts, indicating renal maturation and de novo acquisition of urine-concentrating ability (supplemental online Fig. 3C). Unsurprisingly, UT-B mRNA was detected in both control and repopulated LNs because its expression in erythrocytes and other nonrenal tissues is well-documented [25]. Erythropoietin production was also confirmed in 6-week grafts by RT-PCR analysis of mRNA isolated from phlebotomized mice.

In some mice, all nephrons were morphologically mature by 12 weeks. These nephrons showed glomerular expression of podoplanin and CD31 (Fig. 2A, upper panel). CD31 staining also indicated that ectopic nephrons were vascularized by host arterioles (Fig. 2A, lower panel). Type IV collagen was localized at glomerular basement membranes, tubules (Fig. 2A, upper panel), and the glomerular mesangium (Fig. 2A, lower panel). Because type IV collagen did not always colocalize with GFP^+ cells, it likely originated from both recipient and donor cells. Ectopic nephrons also showed cytokeratin-8- and erythropoietin-positive tubules (Fig. 2A, upper panel; additional erythropoietin staining pictures are shown in supplemental online Fig. 1B).

Kidney grafts were viable and apparently functional at 12 weeks in some mice; however, other mice sacrificed at the same time point revealed grafts comprised of fluid-filled cysts. In particular, three out of eight grafts examined 12 weeks post-transplantation presented mature nephrons, whereas the remaining five showed cysts. We characterized two representative cysts (Fig. 2B). Cyst 1 was lined by a simple squamous epithelium, with apical expression of the water channel aquaporin 1 (AQP1) and the absence of sodium-potassium-chloride transporter 2 (NKCC2), indicating the thin descending limb of Henle's loop as the possible origin (Fig. 2C, left panel). The epithelium was

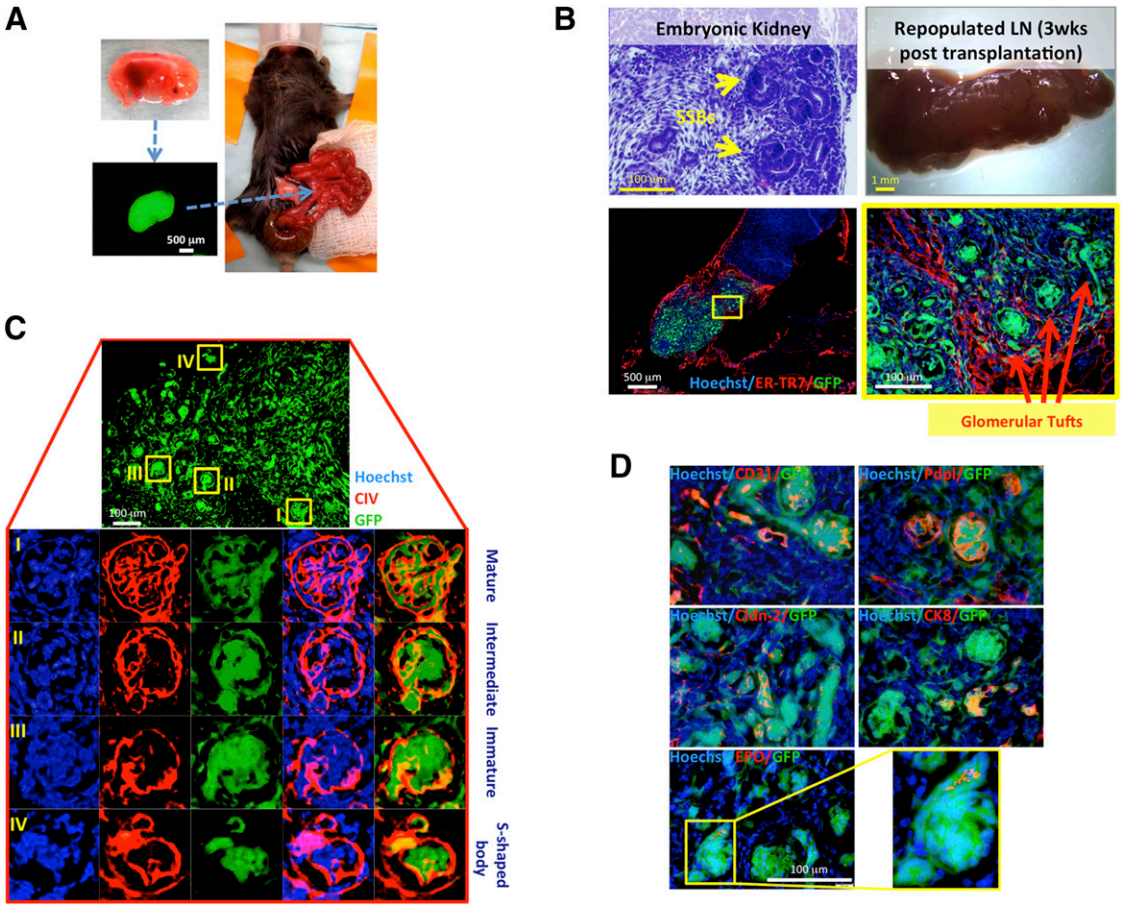

Figure 1. LNs are permissive sites for kidney organogenesis. **(A):** Schematic view of embryonic kidney transplantation into the jejunal LN. **(B):** Hematoxylin and eosin-stained section of donor embryonic kidney showing SSBs (upper left panel); whole-mount LN 3 weeks after embryonic kidney fragment transplantation (upper right panel); and sectional view of the same LN after staining with ER-TR7 (red), with the presence of GFP^+ (green) donor cells. Nuclei were counterstained using Hoechst (blue) (lower left panel). The boxed area is shown enlarged (lower right panel). **(C):** Detail of 3-week kidney graft showing variable glomerular maturity (upper panel). Enlarged views of the boxed regions are shown upon CIV staining (red). Nuclei were counterstained using Hoechst (blue) (lower panels). **(D):** Merged images of GFP (green); CD31, Pdpl, Cldn-2, CK8, or EPO (red); and Hoechst (blue) staining on sections of a 3-week kidney graft. Abbreviations: CIV, collagen IV; CK8, cytokeratin-8; Cldn-2, claudin-2; EPO, erythropoietin; ER-TR7, reticular fibroblasts and reticular fibers; GFP, green fluorescent protein; LN, lymph node; Pdpl, podoplanin; SSBs, S-shaped bodies; wks, weeks.

negative for BrdU, indicating that cyst expansion had already ceased at the time of LN collection (Fig. 2C, left panel). Henle's loop plays a role in ion and water transport, allowing urine production. Accordingly, cyst 1 contained several urinary crystals (Fig. 2E), apart from some eosinophilic proteinaceous material (Fig. 2D, left panel). Crystal shapes included amorphous, oval to round, rhomboid, and parallelepiped, with poorly or sharply defined contours, reaching up to 100 μm in length (Fig. 2E).

Differing from cyst 1, cyst 2 was lined by a simple tall cuboidal epithelium surrounded by collagenous stroma (TRI), with apical endocytic vacuoles, as well as a PAS^+ brush border, possibly originating from proximal convoluted tubule (Fig. 2C, right panel). Accordingly, the epithelium stained positive for AQP1 and negative for AQP2 (Fig. 2C, right panel). Moreover, it showed some BrdU incorporation, indicating that cyst expansion was ongoing at the time of LN collection (Fig. 2C, right panel). The proximal convoluted tubule reabsorbs large molecules, such as proteins. Accordingly, cyst 2 contained pale eosinophilic round globules, 1–20 μm in diameter, that might represent protein globules (Fig. 2D, right panel). These structures are likely hyaline casts covered with fat droplets, indicating glomerular basement membrane injury.

A small cyst with all the features of cyst 2 was also identified (cyst 3; supplemental online Fig. 4A). A mix of GFP^+ and GFP^- cells lined this cyst, indicating a possible hybrid origin.

Structural glomerular alterations could be observed together with cysts. Specifically, histological analyses often revealed compressed tuft surrounded by a circumferential cellular crescent (H&E; supplemental online Fig. 4B, upper panel) with a clear space between tuft and crescent. A mild focal thickening of glomerular basement membranes was observed (PAS; supplemental online Fig. 4B, upper panel), which could be attributed to increased collagen accumulation (TRI and PSR; supplemental online Fig. 4B, upper panel). The cellular crescent contained some $BrdU^+$ cells, indicating active proliferation (supplemental online Fig. 4B, upper panel). Mesangial matrix expansion was confirmed in these glomeruli by intense type IV collagen staining (supplemental online Fig. 4B, upper panel). Hypercellularity within the glomerular tuft, obliterating Bowman's space, was also observed

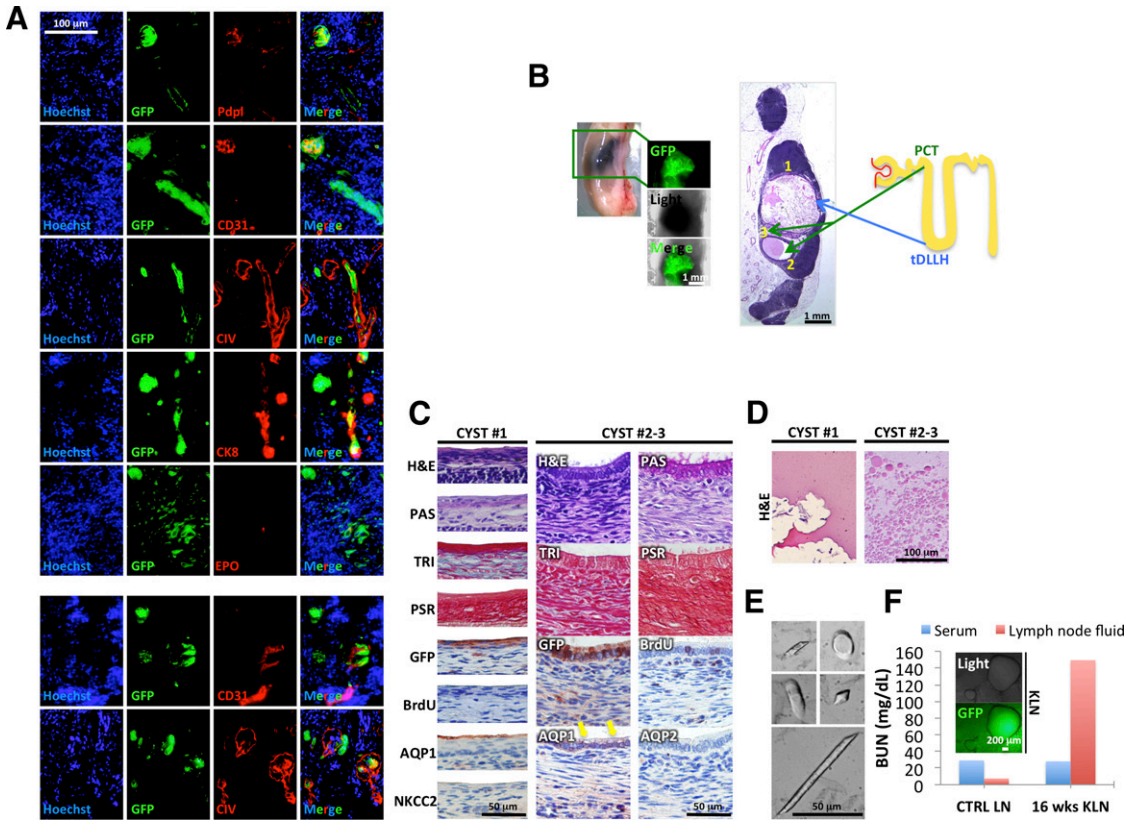

Figure 2. Different outcome of 12-week kidney grafts inside the LNs. **(A):** Immunofluorescence staining of Pdpl, CD31, CIV, CK8, and EPO (red) on sections of 12-week kidney graft (donor cells GFP$^+$, green). Nuclei were counterstained using Hoechst (blue). **(B):** Whole-mount LN and H&E staining showing cysts inside a 12-week kidney graft (left panels) and cartoon depicting nephron structure and origin of cysts from PCT or tDLLH (right panel). **(C):** Detail of cyst 1 epithelium stained with H&E, PAS, TRI, PSR, GFP, BrdU, AQP1, and NKCC2 (left panels), and of cysts 2 and 3 epithelium stained with H&E, PAS, TRI, PSR, GFP, BrdU, AQP1 and 2 (right panels, yellow arrows indicate vacuoles). 3-Amino-9-ethylcarbazole (brown staining) was used to identify targets by immunohistochemistry. **(D):** Details of proteinaceous material found inside cyst 1 (left panel) and of round globules found inside cysts 2 and 3 (right panel) after H&E staining. **(E):** Pictures of urinary crystals found inside cyst 1. **(F):** Blood urea nitrogen levels in serum and LN fluid of a transplanted (16 weeks KLN) *versus* a control mouse. Abbreviations: AQP1, aquaporin 1; BrdU, bromodeoxyuridine; BUN, blood urea nitrogen; CIV, collagen IV; CK8, cytokeratin-8; CTRL, control; EPO, erythropoietin; GFP, green fluorescent protein; H&E, hematoxylin and eosin; KLN, kidney lymph node; LN, lymph node; NKCC2, sodium-potassium-chloride transporter 2; PAS, periodic acid-Schiff; PCT, proximal convoluted tubule; Pdpl, podoplanin; PSR, Picrosirius red; tDLLH, thin descending limb of Henle's loop; TRI, Masson's trichrome; wks, weeks.

(supplemental online Fig. 4B, lower panel). Close to these glomeruli, swelling and vacuolization of proximal tubular cells leading to narrowing of tubular lamina (osmotic nephrosis) were detected (supplemental online Fig. 4B, lower panel).

Finally, because urea is removed from the blood by kidneys and excreted in the urine, we measured urea nitrogen in 16-week grafts as readout of ectopic kidney functionality. Indeed, we hypothesized that if the ectopic kidneys were functional, that is, able to filter the blood and produce wastes, and if these wastes could not be eliminated from the LN, we would detect metabolic waste products including urea within the graft. Although serum urea nitrogen levels were not altered in transplanted mice as compared with control mice, they were highly elevated in LN fluid after kidney transplantation and cyst formation (Fig. 2F). However, urea nitrogen levels were not increased in engrafted LNs where no macroscopic cysts could be observed (data not shown), further indicating that the time window of ectopic kidney maturation differs greatly among mice. Taken together, our study shows the first long-term survival of metanephroi transplanted into an ectopic site.

Bone Marrow-Derived Host Cells Integrate Into the Developing Tissue

On the basis of the results shown in Figure 2A (lower panel) and supplemental online Figure 4A, we hypothesized that kidney organogenesis inside the LN could be attributed to the combination of transplanted kidney stem/progenitor cells and stem/progenitor cells of host origin such as bone marrow.

To investigate whether bone marrow contributes to kidney organogenesis within the LN, GFP bone marrow chimeras were generated. Bone marrow engraftment was monitored by cytometric analysis of peripheral blood 6 weeks after irradiation and cell transplantation (Fig. 3A). All mice except one showed $>$75% of GFP$^+$ leukocytes in their blood (Fig. 3B). The mouse showing the lowest engraftment (bone-marrow transplanted mouse 5) died 8 weeks following transplantation and was excluded from this study. Lymphocyte and granulocyte/monocyte subpopulations were also determined using a basic antibody panel. Gating strategy is indicated in supplemental online Fig. 5A. Briefly, within the GFP$^+$CD45$^+$ cell population, 13.8% $\pm$ 5.1%

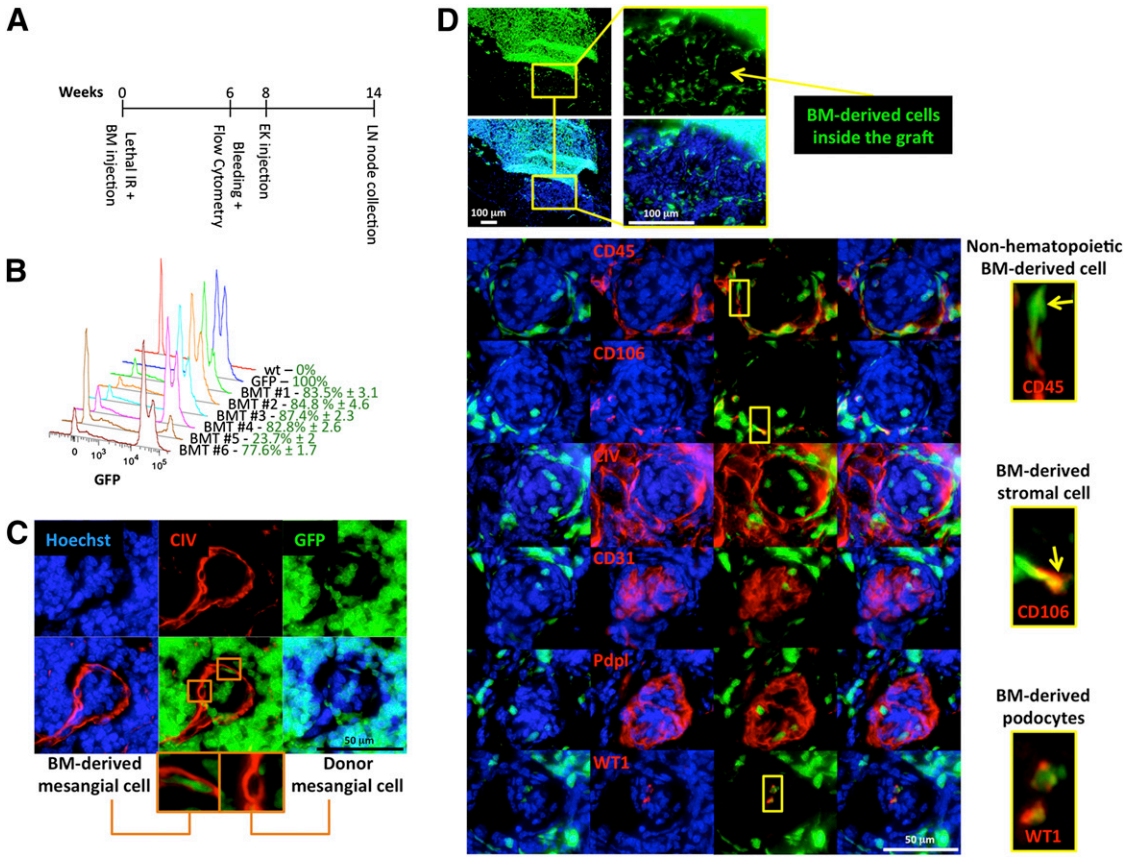

Figure 3. Host bone marrow-derived cells contribute to mesangial and podocyte regeneration. **(A):** Overview of experimental plan. Following lethal IR, wt mice were immediately retro-orbitally infused with GFP^+ bone marrow cells. Donor engraftment was monitored 6 weeks after transplantation by flow cytometric analysis of the peripheral blood. Following 2 additional weeks, bone marrow chimeric mouse LNs were injected with wt embryonic kidney fragments. Mice were sacrificed 6 weeks later for analysis. **(B):** Fluorescence intensity profiles of GFP^+ leukocytes in peripheral blood of a representative group of bone marrow chimeric mice 6 weeks after transplantation. Blood of a wt mouse and that of a GFP^+ mouse were used as negative and positive controls, respectively. **(C):** Representative 6-week ectopic glomerulus grown inside LNs of GFP bone marrow chimeric mice, showing bone marrow-derived contribution to glomerular mesangium. Sections were stained for CIV (red), and nuclei were counterstained using Hoechst (blue). **(D):** Pictures of an LN section from a bone marrow chimeric mouse showing localization of GFP^+ bone marrow-derived cells in a 6-week kidney graft (upper panels). Representative ectopic glomeruli as in **(C)** (lower panels). Sections were stained with CD45, CD106, CIV, CD31, Pdpl, or WT1 (red); nuclei were counterstained using Hoechst (blue). Insets show the presence of GFP^+CD45^-, GFP^+CD106^+, or GFP^+WT1^+ cell subsets inside ectopic glomeruli. Abbreviations: BM, bone marrow; BMT, bone marrow transplanted mouse; CIV, collagen IV; EK, embryonic kidney; GFP, green fluorescent protein; IR, irradiation; LN, lymph node; Pdpl, podoplanin; wt, wild-type; WT1, Wilms' tumor.

were $CD3^+$ cells; in turn this population was comprised of 61.6% ± 8.7% $CD4^+$ and 8.7% ± 1.5% $CD8^+$ cells. When looking at B-lymphocytes, we found 40.2% ± 9.9% GFP^+CD45^+ cells to be $CD19^+B220^+$ (supplemental online Fig. 5B). Finally, 73.3% ± 15% of total Ly6G and Ly6C were GFP^+ (supplemental online Fig. 5C).

Eight weeks following bone marrow transplantation, all mice received injection of wt embryonic kidneys (Fig. 3A). Bone marrow-derived type IV collagen-producing cells incorporated in developed renal corpuscles (Fig. 3C). Immunofluorescence staining for hematopoietic and nonhematopoietic markers revealed that most GFP^+ cells in the glomeruli were neither lymphocytes nor macrophages (supplemental online Fig. 6). Interestingly, both GFP^+CD45^- and GFP^+CD106^+ cell subsets localized in ectopic glomeruli, suggesting the participation of bone marrow-derived mesenchymal stromal cells in ectopic kidney organogenesis (Fig. 3D). Moreover, glomerular GFP^+/Wilms' tumor $(WT1)^+$ cells were observed, suggesting that bone marrow-derived cells can contribute to ectopic podocyte regeneration (Fig. 3D). Bone marrow-derived cells did not contribute to ectopic graft vascularization, because no GFP^+ cells were incorporated in $CD31^+$ vessels (Fig. 3D). Similarly, bone marrow-derived cells did not contribute to the formation of kidney tubules (data not shown), according to previous observations [26]. Taken together, our findings suggest the generation of a chimeric organ inside the LN.

Nephrectomy Accelerates Kidney Organogenesis

To assess whether the ectopic kidney could proliferate in response to growth stimuli, we performed left nephrectomy 12 days after kidney injection into the LN and added BrdU to the drinking water of recipient mice as indicated in Figure 4A. The number of $BrdU^+$ nuclei per renal cross-section was significantly increased in the contralateral kidneys of nephrectomized animals (Fig. 4B). Ectopic kidneys isolated from both sham-operated and nephrectomized mice showed a variable proliferation rate (data not shown). Importantly, grafts from mice undergoing nephrectomy, collected 3.7 weeks after kidney transplantation, were

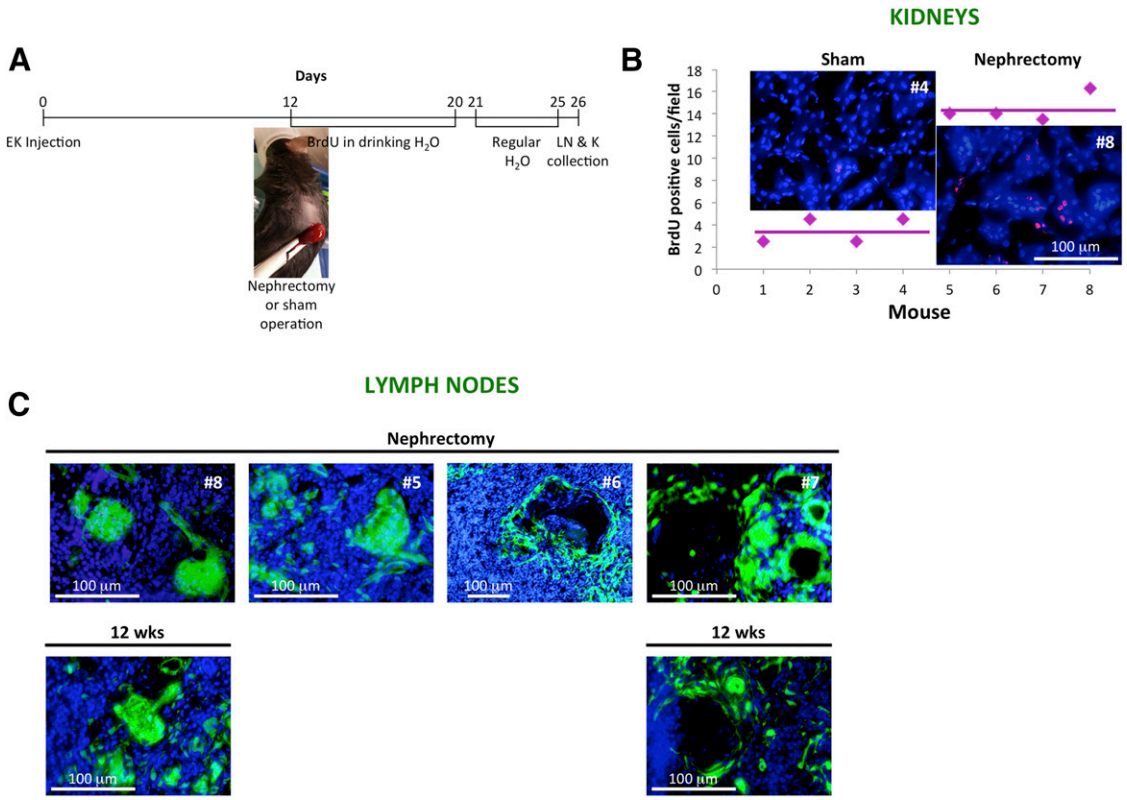

Figure 4. Nephrectomy accelerates kidney organogenesis and degeneration. **(A):** Overview of experimental plan. Twelve days after embryonic kidney transplantation, mice were subjected to the removal of one kidney or a sham operation. All mice were given drinking water containing 0.8 mg/ml BrdU immediately after surgery. BrdU-containing water was prepared fresh and replaced daily for 9 consecutive days, after which it was replaced with regular water. Following 5 additional days, all mice were euthanized for analysis, and LNs and native kidneys collected. **(B):** Dot plot comparing the number of BrdU label-retaining cells in control (mice 1–4) versus remnant kidneys after nephrectomy (mice 5–8). The number of $BrdU^+$ cells was estimated using at least six different randomly selected microscopic fields. Representative immunofluorescence pictures are shown. Sections were stained for BrdU (red), and nuclei were counterstained using Hoechst (blue). **(C):** Representative pictures of 3.7-week kidney grafts of nephrectomized mice (upper panels) as compared with 12-week kidney grafts (lower panels). Abbreviations: BrdU, bromodeoxyuridine; EK, embryonic kidney; K, kidney; LN, lymph node; wks, weeks.

comparable to the 12-week ectopic grafts shown in Figure 2 and supplemental online Figure 4B. In both instances, grafts were comprised of fully mature, apparently healthy nephrons or enlarged and swollen glomeruli (Fig. 4C; supplemental online data includes detailed numbers of cystic alterations).

Although the stimulus that results in compensatory renal growth following renal mass reduction is unnecessary for kidney organogenesis within the LN, nephrectomy accelerates ectopic kidney maturation and possibly degeneration. In our opinion, this reinforces our hypothesis that ectopic kidney degeneration is a consequence of functionality rather than a result of aberrant kidney development. Moreover, because native renal tissue needs to be removed to successfully grow metanephroi in the omentum [9], our findings suggest the LNs might provide a much better site than omentum for ectopic kidney organogenesis.

Whole Kidney Single-Cell Suspensions Self-Organize Into Glomerular/Nephron-Like Structures Within the Lymph Node

Next, we asked whether single-cell suspensions of embryonic kidney could organize into complex specialized components within the LN. Cells were obtained as described in Materials and Methods, and injected into the LNs of 11 recipient mice. Sixteen hours later, analysis of one injected LN revealed that cells had already organized into clusters (supplemental online Fig. 7A, left panels). The remaining mice were divided into 2 groups and sacrificed 6 or 12 weeks later. Four of five mice in each group showed engraftment. Six-week grafts of embryonic kidney single-cell suspensions contained only a few glomerular/nephron-like structures (supplemental online Fig. 7A, right panels). These structures were surrounded by type IV collagen; were reactive against podoplanin; were poorly vascularized, as indicated by CD31 staining; and contained $WT1^+$ host cells (supplemental online Fig. 7B). Six-week grafts also contained tubular-like structures often showing luminal cytokeratin-8 expression (supplemental online Fig. 7C). Again, few cytokeratin-8^+ cells lining these tubules were of host origin. The number of glomerular/nephron-like structures profoundly increased in 12-week grafts. However, embryonic kidney single-cell suspension-derived glomeruli were poorly vascularized (Fig. 5A, middle panels), although grafts showed several host and/or donor-derived $CD31^+$ vessels (Fig. 5A, lower panels). Nephron-like structures did not express WT1, although they were reactive for podoplanin (Fig. 5B). Moreover, they showed a normal (Fig. 5B, lower panels) or abnormal (Fig. 5C) type IV collagen deposition all along the glomerular

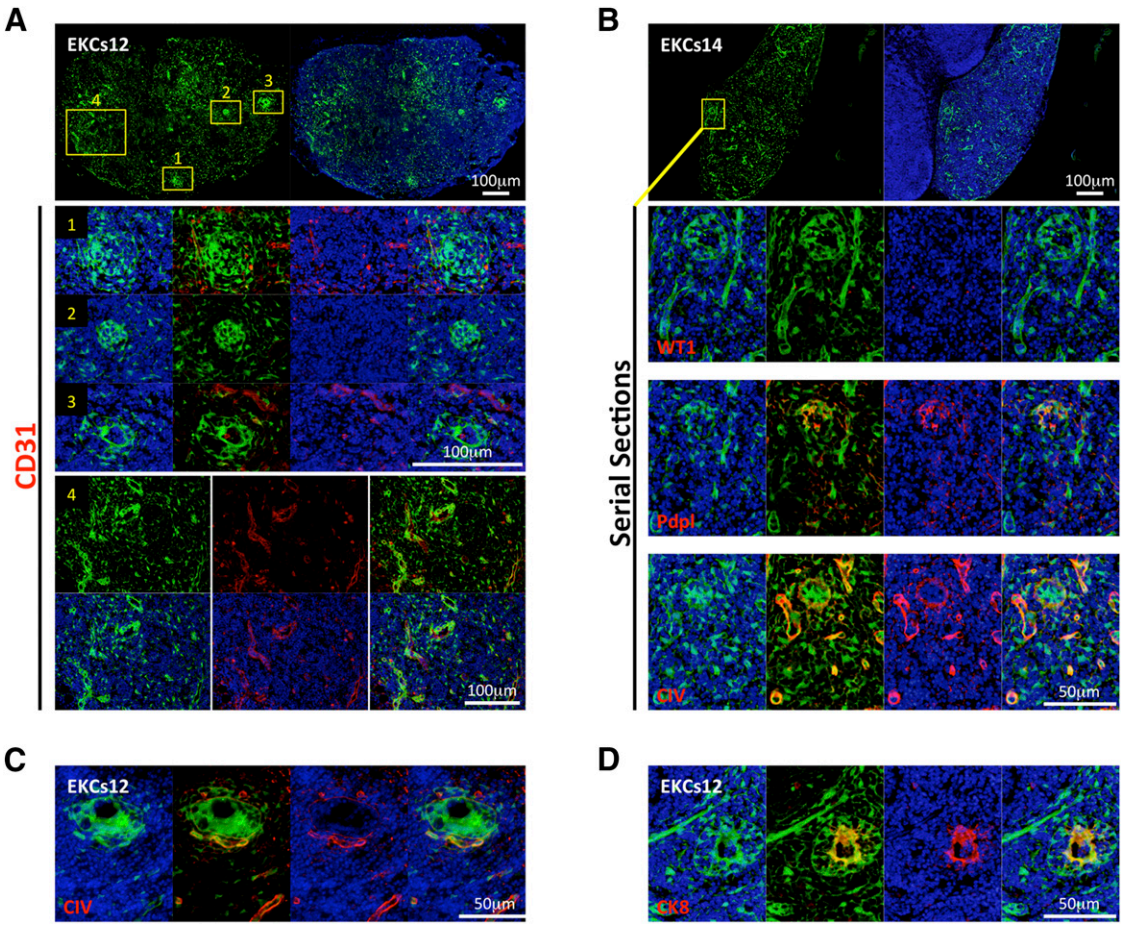

Figure 5. Whole embryonic kidney single-cell suspensions self-organize into glomerular/nephron-like structures within the LN. **(A, B):** Pictures of LN sections with the presence of GFP^+ (green) donor cells 12 weeks after embryonic kidney single-cell suspension injection; nuclei were counterstained using Hoechst (blue) (upper panels). Enlarged views of the boxed regions of staining for CD31 (**[A]**, middle and lower panels) or WT1, Pdpl, and CIV (**[B]**, lower panels) (red) are shown; nuclei were counterstained using Hoechst (blue). **(C, D):** Immunofluorescence staining for CIV or CK8 (red) of LN sections as in **(A, B)**. Nuclei were counterstained using Hoechst (blue). Abbreviations: CIV, collagen IV; CK8, cytokeratin-8; EKCs, embryonic kidney cell suspension; Pdpl, podoplanin; WT1, Wilms' tumor.

basement membranes and/or Bowman's capsule. Furthermore, cytokeratin-8^+ cells were found inside these glomeruli, indicating signs of glomerulosclerosis (Fig. 5D), although no massive immune cell infiltration was detected, as suggested by CD45 staining (supplemental online Fig. 8, upper panels). AQP1 and AQP2 expression was occasionally detected in tubular structures (supplemental online Fig. 8, middle panels). Finally, Ki67 staining revealed that donor cells were not proliferating (supplemental online Fig. 8, lower panels). Taken together, although embryonic kidney single-cell suspension-derived grafts are probably not functional in our model, the LNs might be exploited to understand how different kidney cell types interact and organize into specific structures.

The Lymph Node Might Be Used to Validate the Differentiation Potential of Candidate Stem Cells in Regenerative Nephrology

Next, we sought to investigate the differentiation potential of in vitro-cultured putative mouse renal progenitors inside the LNs. Freshly isolated embryonic kidney cells were plated on a feeder layer and exposed to factors playing a role in pluripotency and differentiation, including factors modulating retinoic acid or Wnt/β-catenin pathway. These pathways can be considered metanephric regulatory signals. Indeed, retinoic acid and retinoic acid receptor agonist treatments stimulate growth and differentiation of mouse metanephric organ cultures [27], induce pronephric tissues in vitro from amphibian ectoderm [28–30], and induce renal lineages from pluripotent stem cells in combination with other factors including the Wnt/β-catenin pathway activator CHIR99021 [31–33]. Among other Wnt activators, RSPOs are likely required for early organogenesis of mouse kidney, as suggested by a few studies investigating RSPO expression changes over developmental stages [34] or the effect of RSPO gene knockout in kidney development [35]. The addition of RSPOs constitutes an absolute requirement for intestinal stem cell cultures [36]. We speculated that immature kidney cell cultures would have similarly benefited from RSPO administration. Because RSPO2 is known to have a stronger signaling potency with respect to other RSPO family members [37], we wanted to investigate its effect on our feeder layer-based embryonic kidney cell culture. In parallel, we investigated the effect of combination of the retinoic acid

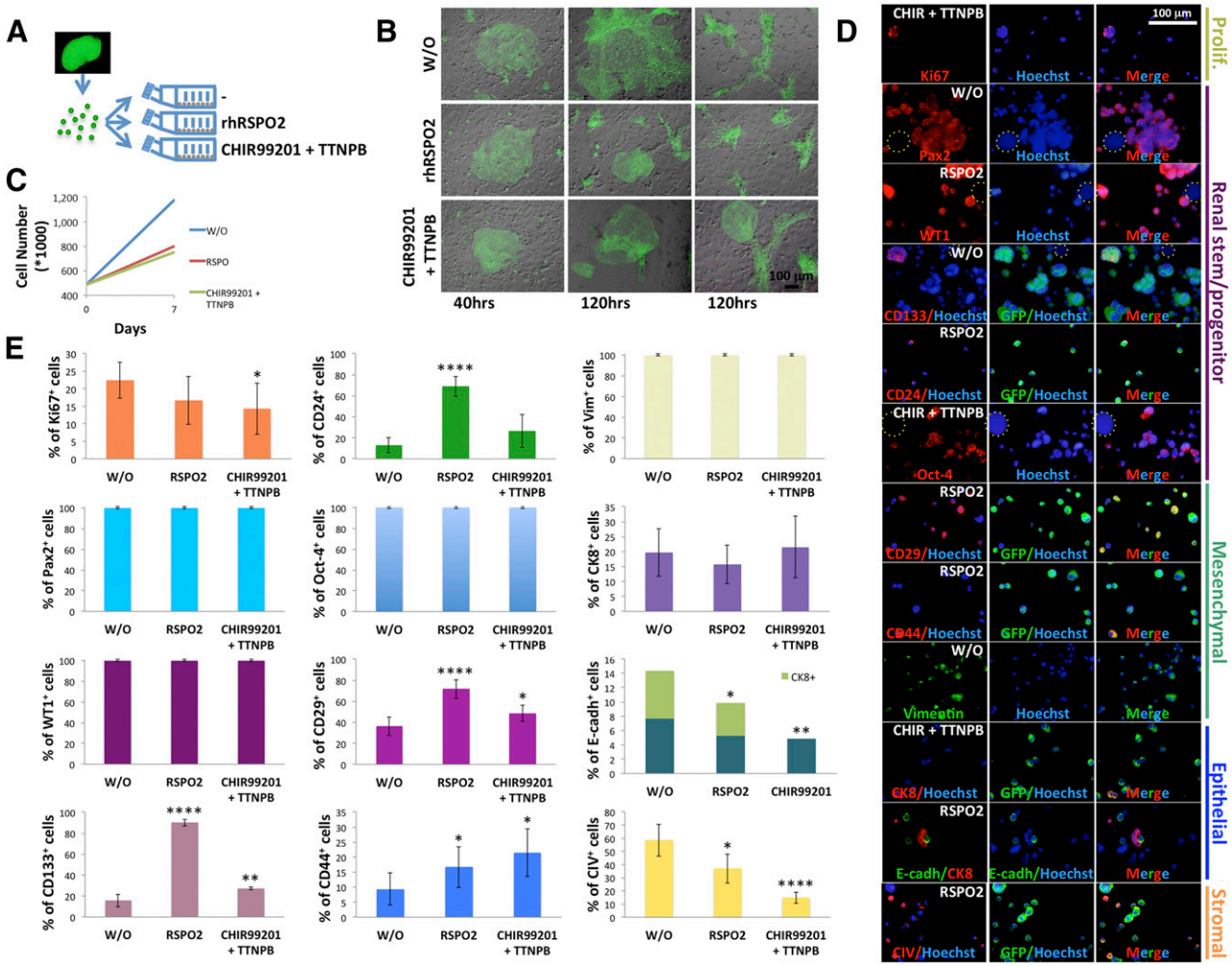

Figure 6. In vitro expansion of mouse renal progenitor cells. **(A):** Schematic diagram illustrating culture of freshly isolated GFP$^+$ embryonic kidney cells. Briefly, after isolation, single embryonic kidney cells were added to T25 flasks containing a confluent feeder layer and treated with or without 100 ng/ml RSPO2 or a combination of 3 μM CHIR99021 and 1 μM TTNPB. **(B):** Merged GFP and bright-field images of embryonic kidney cells growing on feeder layers under different culture conditions at 40 and 120 hours. **(C):** Line graph showing embryonic kidney cell numbers after a 7-day treatment with or without RSPO2 or CHIR99021/TTNPB. **(D):** Representative immunocytochemical stainings for Ki67, Pax2, WT1, CD133, CD24, Oct-4, CD29, CD44, vimentin, CK8, E-cadh, or CIV on embryonic kidney cells after a 7-day treatment as in **(C)** (only one treatment is shown for each marker; dotted circles indicate feeder cells). **(E):** Bar graphs showing the frequency of markers in embryonic kidney cells after a 7-day treatment as in **(C)** (for each marker, percentages of positive cells were determined by averaging up to 14 different randomly selected $\times$20 microscopic fields of immunocytochemical stainings). *, $p < .05$; **, $p < .01$; ***, $p < .001$; ****, $p < .0001$. Abbreviations: CHIR, CHIR99021; CIV, collagen IV; CK8, cytokeratin-8; E-cadh, E-cadherin; GFP, green fluorescent protein; hrs, hours; Oct-4, octamer-4; Pax2, Paired box gene 2; Prolif., proliferation; RSPO2, R-Spondin 2; Vim, vimentin; W/O, control; WT1, Wilms' tumor.

receptor agonist TTNPB plus CHIR99021, as compared with a control culture (Fig. 6A). Within 40 hours of culture, kidney cells in each of the 3 cultures showed growth into what seemed to be clonally derived colonies (Fig. 6B). No difference in cell proliferation was observed at this stage, as suggested by comparable GFP mean fluorescence intensities among the different groups (data not shown). Over time (120 hours after seeding), two main colony types could be observed in control and RSPO2-treated samples: an irregularly shaped flat colony and a spindle-shaped fibroblastoid colony (Fig. 6B). Colonies were larger in the control sample than the RSPO2-treated sample (Fig. 6B). Interestingly, CHIR99021/TTNPB-treated cells organized into surprisingly nephron-like structures (Fig. 6B). Following 7 days of culture, the cells were detached and counted. Kidney suspensions appeared heterogeneous under the microscope, comprised of variable-sized cells with multiple morphologies. Contrary to expected results, RSPO2- and CHIR99021/TTNPB-treated samples exhibited more than a 30% decrease in cell number compared with the untreated control (Fig. 6C). Three groups of mice received LN injections of control or RSPO2- or CHIR99021/TTNPB-treated cells. Remaining cells were stained for markers of proliferation (Ki67), renal stem/progenitor (paired box gene 2 [Pax2], WT1, CD133, CD24, octamer-4 [Oct-4]), mesenchymal (CD29, CD44, vimentin), epithelial (cytokeratin-8, E-cadherin), or stromal (type IV collagen) cells (Fig. 6D). Although acetone used for cell fixation bleached GFP fluorescence, kidney cells were still easily distinguished from feeder cells based on their smaller size. Nonetheless, when possible, costaining with an anti-GFP antibody was performed. Immunoreactive cells were quantified, and the data were graphed as the percentage of positive cells

out of the total cell number (Fig. 6E). Treated samples showed a lower percentage of Ki67-labeled cells than control samples, although this difference was not significant or was barely significant. Regardless of the treatment, all cells were Pax2$^+$ and WT1$^+$, indicating that the feeder-based/low-serum culture preserved an immature phenotype because these proteins are coexpressed only in the condensing mesenchyme and comma- and S-shaped bodies [38]. Although CHIR99021/TTNPB exerted a weak effect on CD133 and CD24 markers, RSPO2 treatment caused a striking increase of both. Regardless of the treatment, all cells showed a strong nuclear Oct-4 expression. Moreover, RSPO2 and CHIR99021/TTNPB treatment similarly modulated CD29 and CD44 expression. Regardless of the treatment, all the cells were vimentin$^+$, another marker of early mesenchyme. When looking at epithelial markers, few cytokeratin-8$^+$ and E-cadherin$^+$ cells were observed in all three samples. Approximately half of the E-cadherin$^+$ cells also expressed cytokeratin-8 in both control and RSPO2-treated samples, whereas no E-cadherin$^+$/cytokeratin-8$^+$ cells were found in the CHIR99021/TTNPB cell group. Finally, type IV collagen$^+$ cells were significantly reduced following both treatments.

Mice receiving LN injection of control or RSPO2- or CHIR99021/TTNPB-treated embryonic kidney cells were divided in 2 groups and sacrificed 3 or 6 weeks later. Interestingly, we found only RSPO2-treated cells were able to engraft, although both 3- and 6-week grafts were very small. Of note, RSPO2-treated cells gave rise to a monomorphic cell population with a neuronal-like appearance (Fig. 7A). No differences in terms of morphology were observed between the two time points examined. Because podocytes share many features with neurons, we first investigated whether our grafts stained positive for podocyte markers, including podoplanin and WT1. Interestingly, we found grafted cells to be primarily negative for these markers (Fig. 7A). Because candidate kidney stem/progenitor cells can express neural features [39, 40], we hypothesized that the cells seen in grafts derived from RSPO2-treated cells could have been neuron-like cells. We stained these grafts with 200-kDa neurofilament heavy (NF200) marker and found all cells to be positive (Fig. 7B). Interestingly, passaged RSPO-treated cells after a period of quiescence started to rapidly proliferate as neurosphere-like floating aggregates expressing the CD133 stem cell marker, the neural stem and progenitor cell markers Nestin and Sox2 (sex-determining region Y-box 2), and the pluripotency marker Oct-4 (Fig. 7C, upper panels). Attached to feeder cells, neuron-like cells could sometimes be observed (Fig. 7C, lower panels). This pattern was maintained in long-term culture even after RSPO2 deprivation (data not shown). Thus, the LN can be exploited to study the behavior of multiple cell populations with stem/progenitor features. In conclusion, our previous and current findings suggest that LNs can have multiple applications, including restoration of tissue function [20, 21], drug testing [22], developmental studies, disease modeling, and cell fate tracking (Fig. 7D).

Discussion

In contrast to lower vertebrates, mammalian nephrogenesis is limited to gestation and early postnatal life. Although the adult kidney cannot make new nephrons, it can regenerate and recover in some circumstances. However, whereas acute renal insults are handled with successful regeneration, chronic injuries lead to ineffective or even more damaging cellular responses [41].

Embryonic kidney transplantation has been indicated as a potential method to support kidney function [9, 11–13, 42]. However, various hurdles remain before clinical therapy can become a reality. Culture techniques to produce organoids starting from mouse embryonic kidneys have been described, but several attempts to develop functional glomeruli have failed because the avascular in vitro environment does not support glomerulogenesis. Moreover, for clinical use, these organoids would have to come from a human fetus, which would be ethically problematic. Induced pluripotent stem cells (iPSCs) have the potential to overcome ethical concerns surrounding the use of embryonic stem cells. Very recently, both ureteric bud- and metanephric mesenchyme-like cells have been generated from iPSCs [43–45]. However, in these studies, iPSC differentiation was performed in monolayers, possibly an adverse environment for self-organization and morphogenesis. Kidney function not only requires the combined action of various cell types organized into specific segments but also necessitates a special three-dimensional architecture allowing interaction between the luminal ultrafiltrate, tubular epithelial cells, and the interstitial space or peritubular vessels [46]. If the culture conditions do not replicate the niche present within the nephrogenic zone of the developing kidney, then even an appropriate set of reprogramming genes may not induce the target cell type [47]. Therefore, it will be essential to provide the reprogrammed cells with a suitable niche; otherwise the newly established phenotype will be unstable. Our previous [20–22] and current studies indicate the LNs might meet this demand. When embryonic kidney fragments were transplanted into the LNs, host blood vessels integrated into the developing glomeruli suggesting access to the bloodstream, a critical challenge to achieve filtration. Vascularization was likely attributable to migration of resident endothelial cells and did not involve bone marrow-derived cells. However, both bone marrow hematopoietic and stromal cells were found in the ectopic kidney. These cells contributed to mesangial and podocyte regeneration. Importantly, the LNs not only furnished the developing tissue with host cells but also provided it with homeostatic signals, because nephrectomy increased ectopic kidney maturation.

We showed a time-dependent maturation of embryonic kidney fragments within the LN. Although some degree of maturation could be already observed in 3-week grafts, the first mature nephrons did not appear until the 6th week. Until this stage, no histological alterations were detected. However, if nephrectomy was performed in the recipient and grafts were collected within 4 weeks (3.7 weeks, 26 days) from transplantation, fully mature nephrons were observed, indicating that nephrectomy accelerates maturation. Not only were fully mature nephrons observed, but glomerular cysts could also be detected in some mice. This outcome is comparable to the outcome observed in 12-week grafts growing in the absence of a homeostatic signal (i.e., in a healthy recipient), in which both viable and apparently functional nephrons or fluid-filled cysts were observed. In both instances, it is conceivable that as the nephron forms, in a time window that differs based on extrinsic cues provided, it produces fluid waste, which progressively accumulates resulting in degenerative alterations. In hepatized LNs, ectopically produced bile juice is transported by the serum and eventually processed in the native liver without affecting the host [20, 21] (unpublished data). Similarly, kidney fluids and waste might, in some cases, be successfully drained into lymphatic and blood vessels, permitting better survival of the ectopic graft. In other cases,

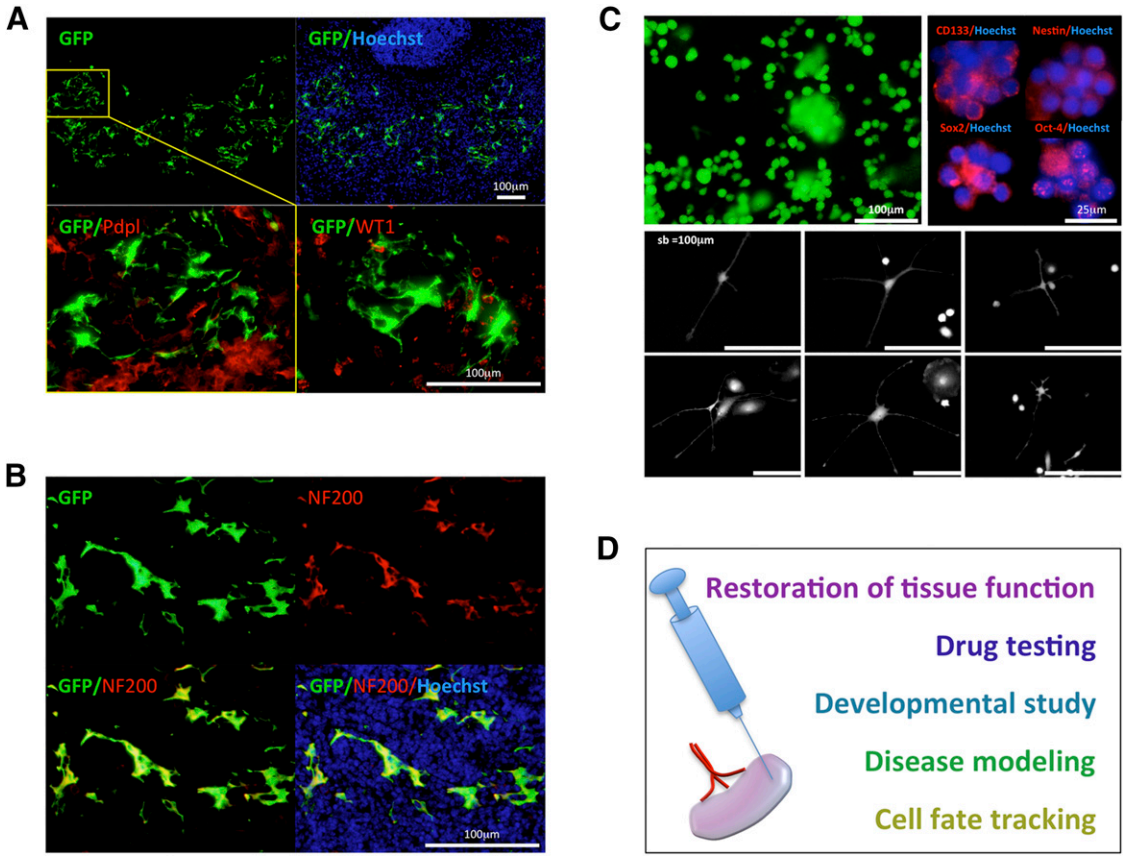

Figure 7. Upon stimulation with R-Spondin 2 (RSPO2), short-term cultured embryonic kidney cells give rise to neuron-like cells expressing NF200 within the LN. **(A):** Picture of an LN section with the presence of GFP^+ (green) donor cells 3 weeks after RSPO2-treated embryonic kidney cell injection; nuclei were counterstained using Hoechst (blue) (upper panels). Enlarged view of the boxed region is shown upon Pdpl staining (red, left lower panel). A serial section was used for WT1 staining (red, right lower panel). **(B):** Picture of an LN section as in **(A)** stained for NF200 (red), with the presence of GFP^+ (green) donor cells; nuclei were counterstained using Hoechst (blue). **(C):** Floating embryonic kidney cell aggregates growing on feeder layers after treatment with RSPO2 (upper left panel). Immunocytochemical staining of floating aggregates for CD133, Nestin, Sox2, and Oct-4 (red); nuclei were counterstained using Hoechst (blue) (upper right panels). The lower panels show neural-like morphology of embryonic kidney-derived adherent cells. **(D):** Schematic diagram illustrating potential applications of the LN. Abbreviations: GFP, green fluorescent protein; NF200, 200-kDa neurofilament heavy; Oct-4, octamer-4; Pdpl, Podoplanin; sb, scale bar; Sox2, sex-determining region Y-box 2; WT1, Wilms' tumor.

kidney products might accumulate inside the tubules, activating epithelial cell proliferation and vectorial fluid secretion, eventually leading to cyst formation. In other words, cyst formation inside the repopulated LN could share some traits with multicystic dysplastic kidney and obstructive dysplasia, in which urinary tract obstructive lesions cause urine retention in functioning nephrons leading to cystogenesis [48].

Although functional organogenesis from embryonic kidney cells is challenging within the LNs because of kidney complexity, we demonstrate that this innovative platform can be exploited to study the behavior of multiple cell populations with stem/progenitor features, as with our RSPO2-treated embryonic kidney cells. RSPOs, a family of secreted proteins, are potent Wnt signal enhancers and stem cell growth factors [49]. In the context of kidney, Wnt signals are mainly known to stimulate uncommitted mesenchymal cells to differentiate into epithelial cells that will form the nephron [50]. Moreover, Wnt signals are activated during repair and regeneration in animal models of acute ischemic injury, indicating a role in regulation of stem cell recruitment and differentiation during the wound repair process [51]. Interestingly, we found short-term cultured embryonic kidney cells stimulated with RSPO2 gave rise to a monomorphic neuron-like cell population expressing the neuronal NF200 marker within the LN. Although we cannot entirely rule out the possibility that these cells originated from a rare neuronal lineage within the kidney cell culture, it is also possible that they originated from renal stem/progenitor cells. Renal stem/progenitor cells have shown a propensity to differentiate into cells exhibiting phenotypic and functional features of neurons under particular culture conditions, in both human and rodent setting [39, 40, 52]. If renal stem/progenitor cells are the cells of origin for the $NF200^+$ cell population found within the LN, it is unclear which cues stimulated them toward a neuronal fate. It is possible that our culture system allowed cells to maintain their immature phenotype or conferred to them a high degree of plasticity. Moreover, Wnt signaling can also play a pivotal role in neural cell specification [53], so it might be possible that treatment with RSPO2 primed renal cells toward neuronal differentiation.

Interestingly, passaged RSPO-treated cells gave rise to neurosphere-like floating aggregates expressing neuronal stem cell marker in vitro. Attached to feeder cells, neuron-like cells could sometimes be observed. Of note, papillary BrdU-retaining

(putative renal stem/progenitor) cells show the same behavior in vitro, that is, they can form spherical aggregates comprising Nestin$^+$ cells and can give rise to neuron-like cells expressing markers of fully differentiated neurons such as class III β-tubulin [52]. Therefore, we suggest that the LNs might be used to study regulation of lineage decisions and functional specialization in populations with stem/progenitor features.

Conclusion

Our study suggests the LNs might be exploited as an in vivo platform for kidney development studies, as well as in vivo validation of the differentiation potential of candidate stem cells in regenerative nephrology. Although we believe that the LN may also provide an exclusive site for kidney organogenesis for therapeutic purposes, we are well aware that our findings will require a number of challenges to be met before being translated into potential clinical applications. Excretion of metabolic wastes, regulation of water, and ion content in the blood are major renal functions, requiring ESRD patients to undergo dialysis. However, the kidney has another important role in maintaining homeostasis in the body by secreting hormones including erythropoietin, calcitriol (vitamin D_3), and renin. It turns out that although the de novo reconstitution of a functional kidney would be of utmost importance in the clinical setting, it cannot be excluded that the creation of a hormone-releasing tissue may also suffice as a therapeutic tool for certain patient populations. It is plausible that kidney endocrine functions could be replaced or sustained by transplanting only one particular renal cell type in an LN.

A future approach will be to assess this technology in large animals, in which LNs adjacent to kidneys could be transplanted and the graft-host ureter connection could be achieved through surgical and/or engineering techniques. Another approach will be to evaluate the potential of LN-grown kidney tissue to compensate for lost kidney functions including hormone production. The ability of orthotopic transplantation of LN-grown nephrons to support renal functions will also be undertaken. These future investigations will hopefully determine whether the LN can be exploited for the in vivo generation of donor tissue for the eventual treatment of ESRD patients.

Acknowledgments

This work was supported by the Ri.MED Foundation (to M.G.F.) and by NIH Grant R01-DK085711 (to E.L.). We thank Junji Komori for helpful hints on surgical procedures and Aparna Rao for performing retro-orbital injection of bone marrow cells in mice. We also thank Lynda Guzik and Aaron DeWard for proofreading and editing.

Author Contributions

M.G.F.: conception and design, financial support, collection and/or assembly of data, data analysis and interpretation, manuscript writing; E.L.: conception and design, financial support, administrative support, final approval of manuscript.

Disclosure of Potential Conflicts of Interest

The authors indicated no potential conflicts of interest.

References

1 Collins AJ, Foley RN, Chavers B et al. United States Renal Data System 2011 Annual Data Report: Atlas of chronic kidney disease & end-stage renal disease in the United States. Am J Kidney Dis 2012;59:e1–e420.

2 Cascalho M, Platt JL. Xenotransplantation and other means of organ replacement. Nat Rev Immunol 2001;1:154–160.

3 DeWard AD, Komori J, Lagasse E. Ectopic transplantation sites for cell-based therapy. Curr Opin Organ Transplant 2014;19:169–174.

4 Smink AM, Faas MM, de Vos P. Toward engineering a novel transplantation site for human pancreatic islets. Diabetes 2013;62:1357–1364.

5 Navarro-Alvarez N, Soto-Gutierrez A, Chen Y et al. Intramuscular transplantation of engineered hepatic tissue constructs corrects acute and chronic liver failure in mice. J Hepatol 2010;52:211–219.

6 Hammerman MR. Renal organogenesis from transplanted metanephric primordia. J Am Soc Nephrol 2004;15:1126–1132.

7 Merani S, Toso C, Emamaullee J et al. Optimal implantation site for pancreatic islet transplantation. Br J Surg 2008;95:1449–1461.

8 Bartholomeus K, Jacobs-Tulleneers-Thevissen D, Shouyue S et al. Omentum is better site than kidney capsule for growth, differentiation, and vascularization of immature porcine β-cell implants in immunodeficient rats. Transplantation 2013;96:1026–1033.

9 Rogers SA, Lowell JA, Hammerman NA et al. Transplantation of developing metanephroi into adult rats. Kidney Int 1998;54:27–37.

10 Dilworth MR, Clancy MJ, Marshall D et al. Development and functional capacity of transplanted rat metanephroi. Nephrol Dial Transplant 2008;23:871–879.

11 Marshall D, Dilworth MR, Clancy M et al. Increasing renal mass improves survival in anephric rats following metanephros transplantation. Exp Physiol 2007;92:263–271.

12 Kim SS, Park HJ, Han J et al. Improvement of kidney failure with fetal kidney precursor cell transplantation. Transplantation 2007;83:1249–1258.

13 Yokote S, Yokoo T, Matsumoto K et al. The effect of metanephros transplantation on blood pressure in anephric rats with induced acute hypotension. Nephrol Dial Transplant 2012;27:3449–3455.

14 Kim HI, Yu JE, Park CG et al. Comparison of four pancreatic islet implantation sites. J Korean Med Sci 2010;25:203–210.

15 Ellis H. The clinical significance of adhesions: Focus on intestinal obstruction. Eur J Surg Suppl 1997;5–9.

16 Abrahamson DR, St John PL, Pillion DJ et al. Glomerular development in intraocular and intrarenal grafts of fetal kidneys. Lab Invest 1991;64:629–639.

17 Hyink DP, Tucker DC, St John PL et al. Endogenous origin of glomerular endothelial and mesangial cells in grafts of embryonic kidneys. Am J Physiol 1996;270:F886–F899.

18 Robert B, St John PL, Hyink DP et al. Evidence that embryonic kidney cells expressing flk-1 are intrinsic, vasculogenic angioblasts. Am J Physiol 1996;271:F744–F753.

19 Kistler AD, Caicedo A, Abdulreda MH et al. In vivo imaging of kidney glomeruli transplanted into the anterior chamber of the mouse eye. Sci Rep 2014;4:3872.

20 Hoppo T, Komori J, Manohar R et al. Rescue of lethal hepatic failure by hepatized lymph nodes in mice. Gastroenterology 2011;140:656–666, e652.

21 Komori J, Boone L, DeWard A et al. The mouse lymph node as an ectopic transplantation site for multiple tissues. Nat Biotechnol 2012;30:976–983.

22 Francipane MG, Lagasse E. Selective targeting of human colon cancer stem-like cells by the mTOR inhibitor Torin-1. Oncotarget 2013;4:1948–1962.

23 Thöny HC, Luethy CM, Zimmermann A et al. Histological features of glomerular immaturity in infants and small children with normal or altered tubular function. Eur J Pediatr 1995;154(suppl 4):S65–S68.

24 Lee HW, Kim WY, Song HK et al. Sequential expression of NKCC2, TonEBP, aldose reductase, and urea transporter-A in developing mouse kidney. Am J Physiol Renal Physiol 2007;292:F269–F277.

25 Timmer RT, Klein JD, Bagnasco SM et al. Localization of the urea transporter UT-B protein in human and rat erythrocytes and tissues. Am J Physiol Cell Physiol 2001;281:C1318–C1325.

26 Duffield JS, Bonventre JV. Kidney tubular epithelium is restored without replacement with bone marrow-derived cells during repair after ischemic injury. Kidney Int 2005;68:1956–1961.

27 Vilar J, Gilbert T, Moreau E et al. Metanephros organogenesis is highly stimulated by vitamin A derivatives in organ culture. Kidney Int 1996;49:1478–1487.

28 Moriya N, Uchiyama H, Asashima M. Induction of pronephric tubules by activin and retinoic acid in presumptive ectoderm of *Xenopus laevis*. Dev Growth Differ 1993;35:123–128.

29 Brennan HC, Nijjar S, Jones EA. The specification and growth factor inducibility of the pronephric glomus in *Xenopus laevis*. Development 1999;126:5847–5856.

30 Osafune K, Nishinakamura R, Komazaki S et al. In vitro induction of the pronephric duct in *Xenopus* explants. Dev Growth Differ 2002;44:161–167.

31 Kim D, Dressler GR. Nephrogenic factors promote differentiation of mouse embryonic stem cells into renal epithelia. J Am Soc Nephrol 2005;16:3527–3534.

32 Song B, Smink AM, Jones CV et al. The directed differentiation of human iPS cells into kidney podocytes. PLoS One 2012;7:e46453.

33 Araoka T, Mae S, Kurose Y et al. Efficient and rapid induction of human iPSCs/ESCs into nephrogenic intermediate mesoderm using small molecule-based differentiation methods. PLoS One 2014;9:e84881.

34 Parma P, Radi O, Vidal V et al. R-spondin1 is essential in sex determination, skin differentiation and malignancy. Nat Genet 2006;38:1304–1309.

35 Nam JS, Park E, Turcotte TJ et al. Mouse R-spondin2 is required for apical ectodermal ridge maintenance in the hindlimb. Dev Biol 2007;311:124–135.

36 Sato T, Vries RG, Snippert HJ et al. Single Lgr5 stem cells build crypt-villus structures in vitro without a mesenchymal niche. Nature 2009;459:262–265.

37 Moad HE, Pioszak AA. Reconstitution of R-spondin:LGR4:ZNRF3 adult stem cell growth factor signaling complexes with recombinant proteins produced in *Escherichia coli*. Biochemistry 2013;52:7295–7304.

38 Ryan G, Steele-Perkins V, Morris JF et al. Repression of Pax-2 by WT1 during normal kidney development. Development 1995;121:867–875.

39 Sagrinati C, Netti GS, Mazzinghi B et al. Isolation and characterization of multipotent progenitor cells from the Bowman's capsule of adult human kidneys. J Am Soc Nephrol 2006;17:2443–2456.

40 Gupta S, Verfaillie C, Chmielewski D et al. Isolation and characterization of kidney-derived stem cells. J Am Soc Nephrol 2006;17:3028–3040.

41 Li Y, Wingert RA. Regenerative medicine for the kidney: Stem cell prospects & challenges. Clin Transl Med 2013;2:11.

42 Clancy MJ, Marshall D, Dilworth M et al. Immunosuppression is essential for successful allogeneic transplantation of the metanephros. Transplantation 2009;88:151–159.

43 Xia Y, Nivet E, Sancho-Martinez I et al. Directed differentiation of human pluripotent cells to ureteric bud kidney progenitor-like cells. Nat Cell Biol 2013;15:1507–1515.

44 Taguchi A, Kaku Y, Ohmori T et al. Redefining the in vivo origin of metanephric nephron progenitors enables generation of complex kidney structures from pluripotent stem cells. Cell Stem Cell 2014;14:53–67.

45 Takasato M, Er PX, Becroft M et al. Directing human embryonic stem cell differentiation towards a renal lineage generates a self-organizing kidney. Nat Cell Biol 2014;16:118–126.

46 Harari-Steinberg O, Pleniceanu O, Dekel B. Selecting the optimal cell for kidney regeneration: Fetal, adult or reprogrammed stem cells. Organogenesis 2011;7:123–134.

47 Hendry CE, Little MH. Reprogramming the kidney: A novel approach for regeneration. Kidney Int 2012;82:138–146.

48 Nagata M, Shibata S, Shu Y. Pathogenesis of dysplastic kidney associated with urinary tract obstruction in utero. Nephrol Dial Transplant 2002;17(suppl 9):37–38.

49 de Lau W, Peng WC, Gros P et al. The R-spondin/Lgr5/Rnf43 module: Regulator of Wnt signal strength. Genes Dev 2014;28:305–316.

50 Davidson AJ. Mouse Kidney Development. Cambridge, MA: StemBook, 2008.

51 Kawakami T, Ren S, Duffield JS. Wnt signalling in kidney diseases: Dual roles in renal injury and repair. J Pathol 2013;229:221–231.

52 Oliver JA, Maarouf O, Cheema FH et al. The renal papilla is a niche for adult kidney stem cells. J Clin Invest 2004;114:795–804.

53 Zechner D, Fujita Y, Hülsken J et al. β-Catenin signals regulate cell growth and the balance between progenitor cell expansion and differentiation in the nervous system. Dev Biol 2003;258:406–418.

See www.StemCellsTM.com for supporting information available online.

